PERGAMON

Applied Geochemistry 16 (2001) 419–436

Applied Geochemistry

www.elsevier.com/locate/apgeochem

Helium and carbon isotope systematics of natural gases from Taranaki Basin, New Zealand

John R. Hulston [a,*,1], D.R. Hilton [b], I.R. Kaplan [c]

[a] *Institute of Geological and Nuclear Sciences, PO Box 31-312, Lower Hutt, New Zealand*
[b] *Isotope Laboratory, Scripps Institution of Oceanography, University of California, San Diego, La Jolla, CA 92093-0244, USA*
[c] *Global Geochemistry Corporation (ZymaX forensics, Inc.), 16921 Parthenia Street, North Hills, CA 91343, USA*

Received 17 August 1999; accepted 9 May 2000

Editorial handling by R. Fuge

Abstract

The chemical and isotopic compositions of gases from hydrocarbon systems of the Taranaki Basin of New Zealand (both offshore and onshore) show wide variation. The most striking difference between the western and south-eastern groups of gases is the helium content and its isotopic ratio. In the west, the Maui gas is over an order of magnitude higher in helium concentration (up to 190 μmol mol^{-1}) and its ^{3}He/^{4}He ratio of 3.8 R_A (where R_A = the air ^{3}He/^{4}He ratio of 1.4×10^{-6}) is approximately half that of upper mantle helium issuing from volcanic vents of the Taupo Volcanic Zone. In the SE, the Kupe South and most Kapuni natural gases have only a minor mantle helium input of 0.03–0.32 R_A and low total helium concentrations of 10–19 μmol mol^{-1}. The ^{3}He/C ratio (where C represents the total carbon in the gas phase) of the samples measured including those from a recent study of on-shore Taranaki natural gases are generally high at locations where the surface heat flow is high. The ^{3}He/CO_2 ratio of the Maui gases of 5 to 18×10^{-9} is higher than the MORB value of 0.2 to 0.5×10^{-9}, a feature found in other continental basins such as the Pannonian and Vienna basins and in many high helium wells in the USA. Extrapolation to zero CO_2/^{3}He and CO_2/C indicates $\delta^{13}C(CO_2)$ values between −7 and −5‰ close to that of MORB CO_2. The remaining CO_2 would appear to be mostly organically-influenced with $\delta^{13}C(CO_2)$ c.−15‰. There is some evidence of marine carbonate CO_2 in the gases from the New Plymouth field. The radiogenic ^{4}He content (He_{rad}) varies across the Taranaki Basin with the highest He_{rad}/C ratios occurring in the Maui field. $\delta^{13}C(CH_4)$ becomes more enriched in ^{13}C with increasing He_{rad} and hydrocarbon maturity. Because ^{3}He/^{4}He is related to the ratio of mantle to radiogenic crustal helium and ^{3}He/C is virtually constant in the Maui field, there is a correlation between R_C/R_A (where R_C = air-corrected ^{3}He/^{4}He) and $\delta^{13}C(CH_4)$ in the Maui and New Plymouth fields, with the more negative $\delta^{13}C(CH_4)$ values corresponding to high ^{3}He/^{4}He ratios. A correlation between ^{3}He/^{4}He and $\delta^{13}C(CO_2)$ was also observed in the Maui field. In the fields adjacent to Mt Taranaki (2518 m andesitic volcano), correlations of some parameters, particularly CO_2/CH_4, C_2H_6/CH_4 and $\delta^{13}C(CH_4)$, are present with increasing depth of the gas reservoir and with distance from the volcanic cone.

1. Introduction

The natural gases of the Taranaki Basin (Fig. 1) were shown by Sano et al. (1987) and Poreda et al. (1988) to have helium with ^{3}He/^{4}He ratios significantly above the atmospheric value of 1.4×10^{-6} (R_A). Of particular note was the wide difference in ^{3}He/^{4}He ratios between the Maui field in the west of the basin containing a substantial proportion of mantle-derived helium (2.9–3.8 R_A), and Kapuni in the east where radiogenic helium (0.17–0.19 R_A) predominates. In this contribution, we present further measurements of helium isotopes and related hydrocarbons for the Maui field in an attempt to understand the variations occurring across the field. In

* Corresponding author.
E-mail addresses: isotope@xtra.co.nz (J.R. Hulston), drhilton@ucsd.edu (D.R. Hilton), irk@zymaxusa.com (I.R. Kaplan).
[1] Present address: Isotope Consulting Limited, 7 Earlston Grove, Lower Hutt, New Zealand.

0883-2927/01/$ - see front matter
PII: S0883-2927(00)00045-7

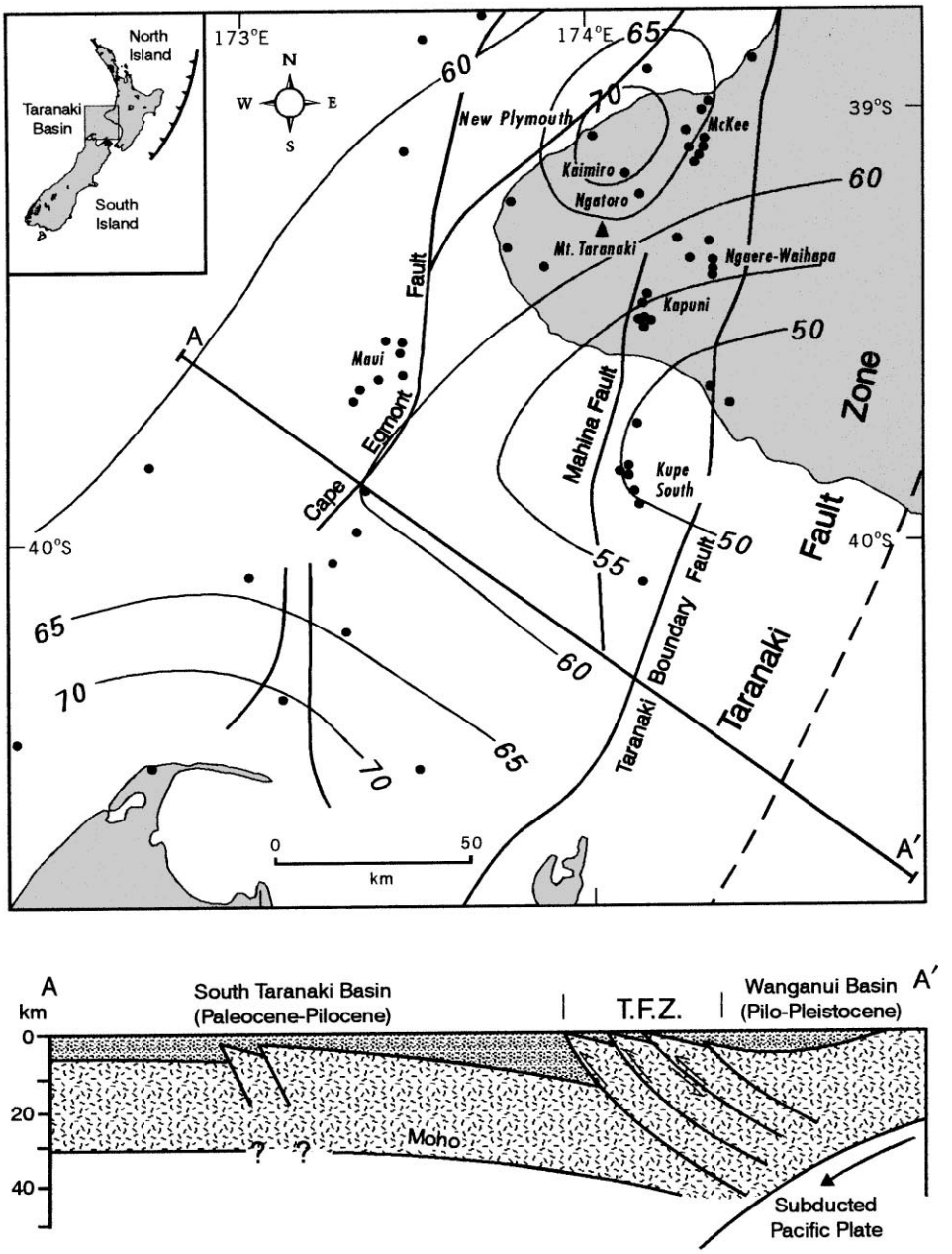

Fig. 1. Map of Taranaki basin showing location of hydrocarbon fields and vents. The surface heat flow (mW m^{-2}) measurements of Funnell et al., 1996) are shown. AA′ the structure of the basement beneath the Taranaki basin as described by Stern and Davey (1990). A thickening of the crust in the SE and extension and thinning in the NW are shown (TFZ, Taranaki Fault Zone).

addition, we have extended the database to include samples from further SE in the basin (Kupe field) and have incorporated data from other Taranaki fields as reported by Lyon et al. (1996).

Poreda et al. (1988) interpreted helium-methane relationships in subduction zone natural gases, including some from the Taranaki Basin, as binary mixtures between a low $^3He/^4He$ (0.01 R_A) ($CH_4/^3He > 10^9$) crustal end member and a high $^3He/^4He$ (3.5 R_A) ($CH_4/^3He < 10^6$) magmatic component. Using a different approach, Sano et al. (1987), argued that high Taranaki Basin $^3He/^4He$ ratios were confined to regions of

high terrestrial heat flow, indicating a common upper mantle origin. Interpreting the helium isotope database, Giggenbach et al. (1993) suggested that either a recent contribution of magmatic helium had occurred at Maui or that the Maui gases had migrated only recently from source areas to the NE — as proposed by Haskell (1991). Lyon et al. (1996) pointed out that the two fields (New Plymouth and Maui) with high $\delta^{13}C(CO_2)$ values are characterised by high $^3He/^4He$ ratios indicating considerable input of helium, and possibly CO_2, from sedimentary sources possibly associated with local andesitic magmatism. In addition, they concluded that the composition of Kapuni gases correspond approximately to that expected for attainment of both chemical and isotopic equilibrium between CO_2 and CH_4 at a temperature of about 150°C. The results were consistent with the CO_2 and CH_4 being derived from a common kerogen source having a $\delta^{13}C$ value of about −27‰. Furthermore, they suggested that much of the variability in CH_4/CO_2 may be due to vapour–liquid separation processes favouring partitioning of CH_4 into the vapour phase and CO_2 into any coexisting aqueous liquid phase.

In this contribution, we have used available chemical and isotopic data together with geological information on the Taranaki Basin which has accumulated over the past decade, to explain the variations of both helium and carbon isotope ratios across the basin and in particular within the Maui field and hence interpret the origin and characteristics of the natural gases. To help accomplish this task, we have used the surface heat flow measurements of Funnell et al. (1996), the organic geochemistry data of Killops et al. (1994) and the geological and geophysical data compiled by King and Thrasher (1996).

1.1. Geology and geophysics of the Taranaki Basin

The presence of condensate in the Taranaki Basin area (Fig. 1) has been known since 1895 but extensive exploration did not begin until the mid-1950s. This resulted in the discovery of two major gas and condensate fields: the onshore Kapuni field in 1959 and the offshore Maui field in 1969. Since then, exploration has continued with the discovery of onshore oil at McKee and Waihapa (1980s) and Ngatoro and Ngaere (1990s), and offshore at Kupe South in the 1980s. In 1984 the ultimate recovery of gas from the Maui field was projected at 2×10^{11} m^3.

The structure of the basement beneath the Taranaki Basin has been described by Stern and Davey (1990) as a thickening of the crust in the SE and extension and thinning in the NW (Fig. 1). From analysis of sub-crustal earthquakes beneath the North Island of New Zealand, Adams and Ware (1977) estimate that the subducting Pacific plate is trending NE–SW at a depth of 150 km beneath the Kapuni field and 200 km beneath Maui. Recently, Funnell et al. (1996) estimated the surface heat flow in the Taranaki Basin to range from 47 mW m^{-2} in the SE to a maximum of 74 mW m^{-2} near New Plymouth (where the subduction zone has a depth of c. 200 km) before decreasing again further to the NW. Their surface heat flow contours are shown in Fig. 1. Earlier views of the geology of the area can be found in McBeath (1977) and Pilaar and Wakefield (1978,1984).

King and Thrasher (1996) summarised current views on the habitat of gas and oil in the Taranaki Basin. The basin is located on the west coast of the North Island in a complex tectonic setting behind the active convergent plate boundary. Like many other composite basins worldwide, its hydrocarbon accumulations are the collective product of several phases of basin evolution. All proven hydrocarbon accumulations occur within a region of pronounced Neogene tectonism, where episodes of uplift and subsequent subsidence followed by sediment burial were particularly significant in the development of source rock maturity and trapping structures. The majority of reserves in Taranaki are contained in late Eocene coastal plain and marginal marine sandstones which were tectonically transformed into structural traps during the Neogene.

Taranaki Basin is an oil, gas, and condensate province. Source rocks for both oil and gas are primarily terrestrial coal measures although biomarkers sometimes reflect kerogen with a marine influence. Thermal modelling and geohistory case studies (e.g. Armstrong et al., 1996) indicate that the thickest sequences of the late Cretaceous source rocks may have started to generate and expel hydrocarbons about 50 to 65 Ma, and that much of the available kerogen has now been depleted. In other areas the source rocks began expelling oil in the mid-late Miocene. Locally Eocene Kapuni Group source rocks also reached the top of the oil expulsion window in the late Miocene. Geochemical signatures are consistent with a Kapuni source component in some produced oils from Taranaki Peninsula wells. Where Kapuni source rocks are mature in the onshore region, maximum rates of hydrocarbon generation coincided with periods of greatest burial in the latest Miocene to early Pliocene. Basin reconstructions indicate that areas of maturity have changed and increased since the Miocene, and that hydrocarbon migration gradients were also significantly different in the late Miocene compared with the Plio-Pleistocene.

Within the Taranaki Basin, hydrocarbon reservoirs have been discovered at all major chrono- stratigraphic levels except for the Cretaceous. Paleogene-aged reservoirs variously contain gas-condensate or oil whereas proven Neogene reservoirs are oil accumulations. Except for one marginally viable field, all economically-producible reserves discovered to date occur above

about 3600 m sub sea. The major fields are not filled to spill, and the maximum gas column thickness of individual reservoirs (at upper Eocene level) is around 200 m.

The bulk of hydrocarbon reserves in Taranaki are contained in single or stacked shoreline and coastal-plain sand reservoirs of Eocene age (Maui, Kapuni, Kaimiro, McKee fields). These Eocene sand depocentres extend diagonally NE–SW across the centre of the basin, parallel to the paleo-shoreline. Miocene turbidity sands deposited at the foot of the continental slope have a similar distribution.

The oldest proven reservoir sequence in Taranaki is the Paleocene Farewell Formation. In the Kupe South field this fluvial sand unit has porosities exceeding 20%. In the Maui field, age-equivalent coastal plain ('F') sands (deeper than those sampled in this study) have porosities in excess of 20%, and constitute the reservoir interval ('F sands') in the recently discovered oil leg in the 'B' Platform vicinity.

The producing 'D Sands' reservoir interval in the Maui field belongs to the early-Eocene Kaimiro Formation. These sands also have porosities in excess of 20%, and are interpreted as tidally-influenced estuarine deposits. Depositional facies indicate an important degree of eustatic control, characterised by transgressive in-filling and back-filling of valley systems that were incised during preceding lowstands. The main 'D1' sand at the top of the reservoir interval is a transgressive barrier facies.

The mid-Eocene Mangahewa Formation, which contains a diverse range of coastal plain, estuarine and shoreline deposits, is a very important reservoir unit in Taranaki. Hydrocarbons have been produced from it in the Maui ('C Sands') and Kapuni. Marginal marine Mangahewa sands in the Maui field have porosities up to 27%. The Mangahewa reservoir interval in the Kapuni field was deposited within a northwest-flowing meandering river system, on a low-relief coastal plain that was subjected to repeated marine incursion.

The McKee Formation is the youngest productive Eocene reservoir. It consists primarily of shallow marine to marginal marine sands, and may be a similar facies to some 'C' sand beds in Maui. The distribution of the McKee Formation appears to be restricted to north-eastern parts of the late Eocene shoreline tract. The formation produces oil in the McKee and Kaimiro fields, in the northern Taranaki Peninsula. In the McKee field, the formation is only 46 m thick, and has porosities of less than 15%.

1.2. Organic geochemistry

King and Thrasher (1996) describe the primary source rocks in the Taranaki Basin as hydrogen-rich coals and carbonaceous mudstones of Late Cretaceous to Eocene age which accumulated in thick sequences in synrift/drift sub-basins and on the post-rift passive margin. A minor marine influence, recorded in the chemistry of most produced oils, is attributed to paralic mudstones interbedded within and immediately overlying the coal measures. The marine contribution is most pronounced towards the NW.

Killops et al. (1994) have shown that it is possible to determine the approximate age of most New Zealand oils from their angiosperm:gymnosperm index (AGI). In general, migration distances appear to be short which has aided identification of specific source units for oils-particularly in the Taranaki Basin. The oils are divided into three families according to their inferred source rock age (Fig. 2). The Maui family of oils are derived from late Cretaceous source rocks, the Kapuni family from Paleocene (or mixed late Cretaceous–Eocene) sources, and the McKee family from an Eocene source. Fig. 2 indicates the Maui oils as the oldest followed by the Kapuni and Kupe S oils with the McKee oils being the youngest. The oils are largely derived from terrestrial plants, but oils from the Maui, Kaimiro and New Plymouth fields also contain a significant marine contribution of organic matter.

Killops et al. (1996) concluded that high levels of CO_2 detected in many petroleum exploration wells on the Taranaki Peninsula can be explained by decarboxylation of vitrinite-rich coals ranging in rank from lignite to early highly volatile bituminous coal. Kinetic modelling of the Kapuni field suggested that CO_2 generation rates from Eocene coals of the Mangahewa Fm. have been high during the last 2 My, with about one half of the generative potential remaining. The oil in the Kapuni field, however, would appear to have been generated from Paleocene coals and the CH_4 from Late Cretaceous Rakopi Formation coals, situated beneath the field. In contrast, in the northern fields of the Taranaki Peninsular, the higher heat flow coupled with a slightly greater burial depth of the Eocene coal measures, has resulted in these Eocene coals reaching peak oil generation earlier, possibly at 5 Ma.

1.3. Analytical procedures

Gas samples, forming part of the present work, were collected in stainless steel cylinders at the pressure of the chiller outlet on the wellhead system of Maui and Kapuni wells. The chiller temperatures and well depths are listed in Table 1. The Kupe South 1 and 2 samples were extracted from the production test samples at depths listed in Table 1. The helium isotope measurement procedure is described by Poreda et al. (1986) and Hilton and Craig (1989). Chemical analyses and carbon isotope measurements were performed using standard techniques at Global Geochemistry Corporation (Jenden and Kaplan, 1989).

Biomarker and surface heat flow data are not available for all wells where gas samples were collected. In

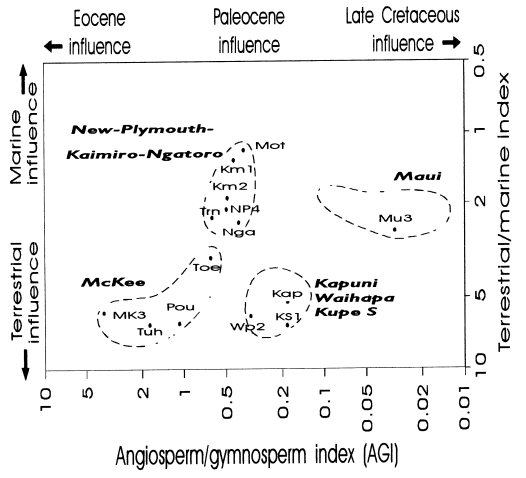

Fig. 2. Biomarker characteristic of Taranaki oils associated with the gases discussed in this paper. Modified (the axes have been rotated to show similarity with Fig. 7) from Killops et al. (1994) and King and Thrasher (1996). The main groups are encircled by dashes. See Table 1 for well abbreviations.

these cases, data from the nearest appropriate site have been used and the correspondence noted in Table 1. In particular, it should be stated that the heat flow and biomarker data for the Maui field are derived from the exploration wells, which were numbered Maui-3 (Mu3), etc., whereas the gas isotope samples have been collected from the Maui-A production platform numbered Maui A-2, etc. The New Plymouth field biomarker data includes samples from the now exhausted Moturoa field (Mot) while the gas data listed in Tables 1 and 2 have been obtained from the Paritutu-1 exploration well and the Motumahanga undersea gas discharge off New Plymouth.

2. Results

Results of chemical and isotopic measurements of the Taranaki gases are shown in Tables 2 and 3. Table 2 includes the helium isotope measurements and the He/Ne ratios relative to the atmospheric ratio $[(He/Ne)_{air}]$. The helium isotope ratios, (R_C/R_A) have been corrected for air addition during collection as follows:

$$R_C/R_A = [(R/R_A)X - 1]/(X - 1) \quad (1)$$

where $X = (He/Ne)_{air}$ for gas samples or $X = 0.82(He/Ne)_{air}$ for fluid samples and $(He/Ne)_{air}$ represents the He/Ne ratio of the sample relative to that of air.

Also listed in Tables 1 and 2 are surface heat flow values estimated from the data of Funnell et al. (1996), and the chemical and isotopic analyses of Taranaki gas phase samples reported by Lyon et al. (1996). We have however omitted the results of the 1993 Maui samples listed by Lyon et al. (1996) because they appear to have come downstream of the production line of the platform gas/condensate separation system (Steffen Ochs, pers. comm., 1998) and hence are not compatible with the other results presented here. Table 3 lists C_4–C_5 chemical analyses and carbon and hydrogen isotopic composition of C_2–C_3 hydrocarbons analysed for this paper. Table 4 lists the regression coefficients (r) for the majority of the data correlations discussed here.

The most striking difference between the Maui and Kapuni/Kupe South groups of gases is in the helium content and isotopic composition. Maui gas contains over an order of magnitude more helium (up to 197 μmol mol^{-1}) and is considerably enriched in ^{3}He. In contrast, Kupe South and most Kapuni natural gases have low helium contents of 10–19 μmol mol^{-1} and low ^{3}He/^{4}He ratios of 0.03–0.32 R_A with the exception of Kapuni-15, for which ^{3}He/^{4}He is slightly higher at 0.57 R_A. A similar observation, excluding Kapuni-15, was reported by Sano et al. (1987). The ^{3}He/^{4}He ratio (R_C/R_A values in Table 2) of Maui gas is over two orders of magnitude higher than in natural gases which have no apparent mantle input and is approximately half that of upper mantle helium isotope measurements of up to 7.4 R_A issuing from volcanic vents in the Taupo Volcanic Zone, New Zealand (Hulston and Lupton, 1986).

3. Discussion

3.1. Relationships to surface heat flow

The most obvious general trends in the results in Table 2 is the significant increase in the ^{3}He/C ratio [where C represents the total carbon in the gas phase, but excluding C_{4+} hydrocarbons for compatibility with the results of Lyon et al. (1996)] across the basin from c. 10^{-12} at Kupe S to c. 10^{-9} in the Maui and New Plymouth areas, confirming the correlation between mantle ^{3}He and surface heat flow. Plots of log(^{3}He/C) and ^{3}He/^{4}He vs. surface heat flow [Fig. 3(a) and (b)] indicate that log(^{3}He/C) has a marginally better relationship (regression coefficient $r = 0.81$) with surface heat flow than with R_C/R_A ($r = 0.78$), although both are significant. The lack of a more linear relationship is not surprising when other variables are considered — specifically, the total carbon (C) in the log(^{3}He/C) ratio comprises a mixture of organic and possibly carbonate and/or mantle sources, with the magnitude of the organic component being dependent on the source rock productivity as well as temperature. Interestingly the correlation for log(^{3}He/CH_4) vs. surface heat flow at $r = 0.83$ (not shown) is similar to that of log(^{3}He/C) vs. surface heat flow, indicating that the rate of ^{3}He release

Table 1
Sampling details

Name	Date (yymmdd)	Surface heat flow (mW m^{-2})	Details	Ref.[a]	Nearest biomarker site
Maui A Platform — C sands					
Maui A-2(N)	840124	64	Natural gas well, C sand	b	Mu3
Maui A-3(P)	880314	64	Collected from cooler at −2°C	a	Mu3
Maui A-4(D)	880314	64	Collected from cooler at −2°C	a	Mu3
Maui A-9(M)	850900	64	Collected from cooler at −5°C	a	Mu3
Maui A Platform — D sands					
Maui A-8(A)	840124	64	Natural gas well, D sand	b	Mu3
Maui A-8(A)	880314	64	Collected from cooler at −5°C	a	Mu3
Kapuni					
Kapuni-4	840120	53	Natural gas well	b	Kap
Kapuni-4	850900	53	Collected from cooler at +10°C	a	Kap
Kapuni-8	840120	53	Natural gas well	b	Kap
Kapuni-11	931109	53	KA-3E reservoir	b	Kap
Kapuni-15	931109	55	KA-1A reservoir	b	Kap
Kupe South					
Kupe S-1	880000	50	DST 3 Gas Cap	a	KS1
Kupe S-2	880000	50	DST 3 Soln. Gas	a	KS1
New Plymouth area — vent and drillhole					
Motumahanga	890327	74	Offshore vent 24 m depth	b	NP4, Mot,Trn
Paritutu-1/375	930822	74	Drillhole 375 m depth	b	NP4, Mot, Trn
Paritutu-1/560	931022	74	Drillhole 560 m depth	b	NP4, Mot, Trn
Paritutu-1/376	930822	74	Drillhole 376 m depth	b	NP4, Mot, Trn
Ngatoro					
Ngatoro-1	931216	67		b	Nga
Ngatoro-2	931216	67	Collected from separator	b	Nga
Kaimiro					
Kaimiro-2	931216	70		b	Km2
Kaimiro-5	930930	70		b	
Kaimiro-5	930914	70		b	
McKee area					
McKee-2	850521	60	Central McKee	b	MK3
McKee-5A	940308	60	Central McKee	b	MK3
Mystone-1	931207	60	SW McKee	b	
Toetoe-2	850521	60	Southern McKee	b	Toe
Toetoe-6	940308	60	Southern McKee	b	Toe
Tuhua-2	840123	60	Northern McKee	b	Tuh
Tuhua-5A	940308	60	Northern McKee	b	Tuh
Waihapa Field					
Waihapa-2	940308	57	Tikorangi Fm, 2990 m, 85°C	b	Wp2

[a] a, this work; b, Lyon et al. (1996).

is more rapid than CH_4 generation under thermal stress. The increase in R_C/R_A with increase in heat flow also illustrates the higher mantle ^3He compared to radiogenic ^4He from U-Th series radioactive decay from minerals either in the source or reservoir rocks.

It is significant that in both Fig. 3(a) and (b) the Maui samples lie above the regression line while Kaimiro, McKee and to some extent Ngatoro fall below. While the errors in the surface heat flow estimate (c. 3 mW m^{-2}) are not sufficient to explain these differences, it is possible that the present day heat flow may not represent the historic heat flow conditions during hydrocarbon gas generation. Allis et al. (1995) have indicated that a contribution of c. 10 mW m^{-2} to the present day heat flow in the Kaimiro and Ngatoro fields might reflect the influence of volcanic flows occurring over the past 0.25 My in the area 15 km to the SW. There are presently no known volcanic sources in the Maui field section of the Tasman Sea which might have caused its historic heat flow to be higher than the present-day heat

Table 2
Chemical (in parts per thousand by volume) and isotopic analyses[a]

Name	Date (yymmdd)	Heat flow (mW m^2)	R_c/R_A	(He/Ne)/(He/Ne)$_{air}$	^{3}He/C (nM M^{-1})	^{3}He/CO$_2$ (mM M^{-1})	He (mM M^{-1})	Ar (mM M^{-1})	N$_2$ (mM M^{-1})	O$_2$ (mM M^{-1})	CO$_2$ (mM M^{-1})	CH$_4$ (mM M^{-1})	C$_2$ (mM M^{-1})	C$_3$ (mM M^{-1})	δ^{13}C (CO$_2$)	δ^{13}C (CH$_4$)	δ^2H (CH$_4$)	Ref.[b]
Maui A Platform — C sands																		
Maui A-2(N)	840124	64	2.93	833	0.683	8.0	0.197	0.164	34	0.7	100	725	71.5	67.6	−13.2	−35.4	−168	b
Maui A-3(P)	880314	64	3.08	247	0.767	17.3	0.190	0.23	37	2.6	47	825	60	22	−10.1	−36.7	−169	a
Maui A-4(D)	880314	64	3.11	249	0.766	16.7	0.190	0.15	30	0.9	49	832	61	22	−10.0	−36.6	−169	a
Maui A-9(M)	850900	64	3.5	2000	0.831	18.0	0.182	0.11	28	0.1	49	830	60	21	−9.8	−37.1	−173	a
Maui A Platform — D sands																		
Maui A-8(A)	840124	64	3.8	1180	0.783	4.76	0.169	0.156	36	1.3	187	646	86.9	43,4	−8.2	−37.2	−173	b
Maui A-8(A)	880314	64	3.8	118	0.781	8.32	0.158	0.17	42	2.3	100	745	67	29	−6.9	−37.9	−170	a
Kapuni																		
Kapuni-4	840120	53	0.17	1390	0.0021	0.0050	0.010	0.020	4		465	437	64.3	31.1	−14.4	−42.3	−192	b
Kapuni-4	850900	53	0.188	400	0.0029	0.0080	0.012	0.020	2.2	0.1	392	515	56	25	−14.4	−42.3	−192	a
Kapuni-8	840120	53	0.19	1840	0.0023	0.0055	0.010	0.118	5		478	423	63.4	31.2	−14.6	−41.2	−199	b
Kapuni-11	931109	53	0.32		0.0041	0.0100	0.010	0.051	8	1.3	448	463	60	20.6		−42.3	−200	b
Kapuni-15	931109	55	0.57	2.7	0.0073	0.0187	0.010	0.242	20	3.7	423	471	60.8	21.1	−14.2	−42.5	−191	b
Kupe South																		
Kupe S-1	880000	50	0.102	140	0.0022	4.48	0.019	0.12	13	2	0.6	798	120	55		−43.3	−203	a
Kupe S-2	880000	50	0.026	10	0.0003	0.098	0.012	0.14	10	1.6	4.4	757	139	67		−42.3	−205	a
New Plymouth Area — vent and drillhole																		
Motumahanga	890327	74	4.89	625	1.07	1.87	0.140	0.789	109	17	507	353	8.9	3.1	−1.3	−39.8	−164	b
Paritutu-1/375	930822	74	4.73		0.324	0.457	0.052	0.048	15	0.8	745	186	35.6	17	−1.0	−40.6	−162	b
Paritutu-1/560	931022	74	4.78	2270	0.455	0.621	0.068	0.056	18	0.6	725	249	4.5	2.7	−0.1	−43.0	−168	b
Paritutu-1/376	930822	74					0.049	0.065	9	1.3	778	198	8.8	4.9	−0.3	−42.0	−170	b
Ngatoro																		
Ngatoro-1	931216	67	1.53	175	0.0627	20.0	0.033	0.55	47	9.3	3.5	816	74.6	49		−36.5	−155	b
Ngatoro-2	931216	67	1.42	1270	0.0443	8.6	0.024	0.063	9	0.7	5.5	919	54.3	11.1		−41.2	−171	b
Kaimiro																		
Kaimiro-2	931216	70	1.3		0.073	1.24	0.045	0.103	10	0	65.4	834	57.7	32.1		−44.7	−170	b
Kaimiro-5	930930	70	1.32								0.3	961	26	13		−47.3	−170	b
Kaimiro-5	930914	70			(0.011)	(6.0)	0.006	0.321	110	26	1.8	792	40.1	29.1		−49.0	−180	b
McKee area																		
McKee-2	850521	60	0.32	7000	0,0041	0.103	0.010	0.152	37	9.6	42.9	805	74.2	31.4		−42.9	−171	b
McKee-5A	940308	60					0.012	0.058	4	0.9	63.4	822	89.3	20.6		−43.0	−170	b
Mystone-1	931207	60	0.51	2000	0.0104	1.03	0.015	0.041	5	0.9	10.3	962	20.6	1.4		−45.5	−173	b
Toetoe-2	850521	60	0.53	1800	0.0373	1.25	0.047	1.60	141	35	27.6	716	54.3	24.3		−40.1	−156	b
Toetoe-6	940308	60					0.016	0.055	5	1.4	54.8	828	88.1	22.6		−41.6	−163	b
Tuhua-2	840123	60	0.4	245	0.0032	0.031	0.007	0.17	4	1.4	125	693	117	59.3	−16.1	−41.3	−170	b
Tuhua-5A	940308	60					0.01	0.047	4	0.7	79	790	102	24.3		−42.8	−169	b
Waihapa field																		
Waihapa-2	940308	57	0.47	250	0.0057	0.042	0.010	0.063	5	1.3	156	723	86.5	27.5		−43.0	−196	b
Accuracy		±2	~3%[c]	±5%	±5%	±5%	±2%	±2%	±2% ±0.1	±2% ±0.1	±2% ±0.1	±2% ±0.1	±2% *0.1	±2% ±0.1	±0.1	±0.1	±2	

[a] See Table 3 for higher hydrocarbons.
[b] a, this work; b, Lyon et al. (1996).
[c] May be slightly higher for samples with (He/Ne)/(He/Ne)$_{air}$ < 100.

Table 3
Chemical and isotopic analysis of higher hydrocarbons (all this work)

Name	Date (yymmdd)	Heat flow (mW m^{-2})	iC_4 (mM M^{-1})	nC_4 (mM M^{-1})	iC_5 (mM M^{-1})	nC_5 (mM M^{-1})	$\delta^{13}CC_2$ (‰)	$\delta^{2}HC_2$ (‰)	$\delta^{13}CC_3$ (‰)	$\delta^{2}HC_3$ (‰)
Maui A Platform — C sands										
Maui A-3(P)	880314	64	3.8	4.3	1.2	0.8	−28.0	−142	−27.1	−146
Maui A-4(D)	880314	64	3.8	4.4	1.2	0.8	−28.1	−147	−17.2	−155
Maui A-9(M)	850900	64	3.8	4.5	1.2	0.8	−29.5	−138	−26.9	
Maui A Platform — D sands										
Maui A-8(A)	880314	64	5.4	7.0	2.1	1.5	−29.5	−142	−28.1	−145
Kapuni										
Kapuni-4	850900	53	5.1	4.0	0.9	0.6	−30.0	−174	−27.7	
Kupe South										
Kupe S-1	880000	50	12.7	9.7	2.7	1.8	−29.5	−163	−27.5	−155
Kupe S-2	880000	50	16	13.4	3.8	2.6	−29.4	−152	−27.7	−147
Accuracy		±2	±2% ±0.1	±2% ±0.1	±2% ±0.1	±2% ±0.1	±0.2	±0.2	±0.2	±2

Table 4
Regression coefficients (r) for Figs. 3–6

Fig.	Relationship	Restrictions	No. points	R
3(a)	Log(^{3}He/C) vs. heat flow	None	24	0.81
3(b)	R_C/R_A vs. heat flow	None	25	0.78
3(b)	R_C/R_A vs. heat flow	Excluding Kaimiro	23	0.86
3(c)	$\delta^{13}C(CO_2)$ vs. heat flow	None	15	0.93
3(d)	$\delta^{2}H(CH_4)$ vs. heat flow	None	30	0.76
3(e)	Log(C_2H_6/CH_4) vs. heat flow	None	30	0.63
3(e)	Log(C_2H_6/CH_4) vs. heat flow	Excluding Mystone-1, Tuhua-5, Kaimiro-5 and N.P.	23	0.84
4(b)	CO_2/C vs. $\delta^{13}C(CO_2)$	New Plymouth only	4	0.79
5(a)	He_{rad}/C vs. $\delta^{13}C(CH_4)$	None	24	0.81
5(a)	He_{rad}/C vs. $\delta^{13}C(CH_4)$	Excluding Mystone-1 (McKee)	23	0.88
5(a)	He_{rad}/C vs. $\delta^{13}C(CH_4)$	$He_{rad}/C > 4\times10^{-5}$	8	0.92
5(b)	R_C/R_A vs. $\delta^{13}C(CH_4)$	Maui and N.P. only	9	−0.91
6(a)	R_C/R_A vs. $\delta^{13}C(CO_2)$	Maui and N.P. only	9	0.98
6(b)	$\delta^{13}C(CH_4)$ vs. $\delta^{13}C(CO_2)$	Maui only	6	−0.98

flow, but the proximity of the Cape Egmont fault may have provided an opportunity for significant leakage of mantle ^{3}He through the thinner crust in this section of the basin (see Fig. 1). This would then explain the high R_C/R_A values in the Maui samples.

Fig. 3(c) and (d) shows the variation of $\delta^{13}C(CO_2)$ and $\delta^{2}H(CH_4)$ with surface heat flow. Both parameters display strong correlations ($r = 0.93$ and 0.76, respectively) with heat flow. One possible explanation for the strong correlation of $\delta^{13}C(CO_2)$ with high heat flow, is that at higher temperatures the production of isotopically light organic CO_2 decreases and CO_2, with $\delta^{13}C$ values close to limestone, may be mobilised under the influence of heat. The explanation for increased values of $\delta^{2}H(CH_4)$ could possibly result from loss of methane by heat driven diffusion. The $\delta^{13}C(CH_4)$ vs. heat flow plot (not shown), however, displays insignificant correlation ($r = 0.32$), indicating that $\delta^{13}C(CH_4)$ is controlled by other factors.

An interesting correlation was also found between $\log(C_2H_6/CH_4)$ and surface heat flow [Fig. 3(e)]. Although the correlation coefficient for all samples is $r = -0.63$, omission of the outliers Mystone-1, Tuhua-2, Kaimiro-5 and New Plymouth increases the significance to $r = -0.88$. From a study of hydrothermal hydrocarbon gases worldwide, Darling (1998) derived the following empirical relationship between C_2H_6/CH_4 and temperature:

$$t\ (^\circ C) = 57.8\ \log(CH_4/C_2H_6) + 96.8 \quad (2)$$

Temperatures calculated from this relationship (138–198°C), shown on the right of Fig 3(e), are at the high range for the maturation of hydrocarbon source materials but above the range of actual reservoir temperatures of 60–120°C. Other aspects of the C_2H_6/CH_4 ratio variations will be discussed below.

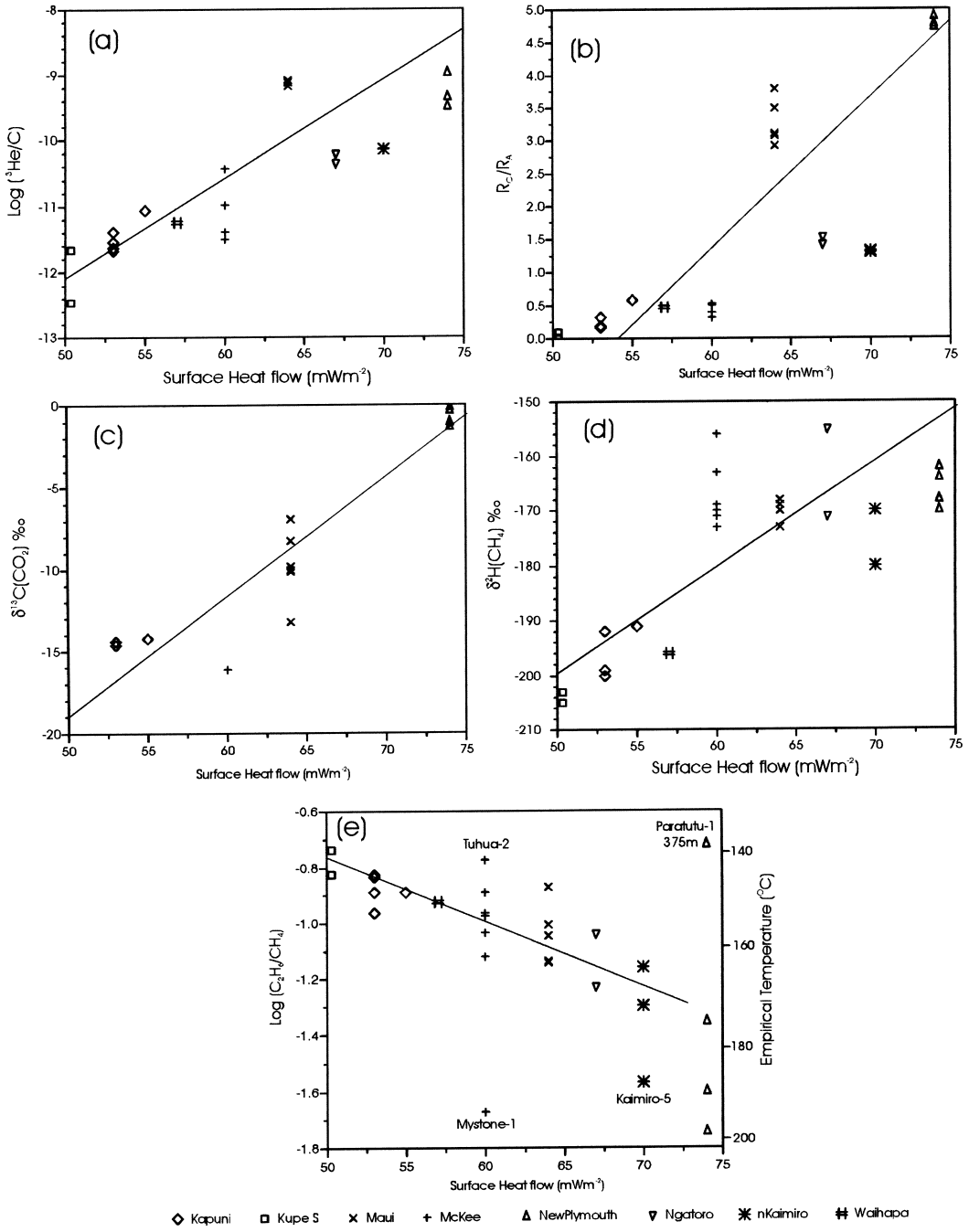

Fig. 3. (a) Log(^{3}He/C) and (b) ^{3}He/^{4}He (R_C/R_A) vs. surface heat flow indicating that log(^{3}He/C) has a marginally better relationship ($r=0.81$) with surface heat flow than R_C/R_A ($r=0.78$). (c) The variation of $\delta^{13}C(CO_2)$ with surface heat flow has fewer points but shows a distinct variation with surface heat flow ($r=0.93$). (d) The plot of $\delta^2H(CH_4)$ against surface heat flow shows an almost step-like function. (e) C_2H_6/CH_4 vs. surface heat flow. The line fit shown ($r=-0.90$) excludes N.P. field and the other three samples labelled. Temperatures calculated from the empirical relationship [Eq. (2)] derived by Darling (1998) are shown on the right axis.

3.2. The fate of mantle carbon and the mantle carbon isotope signature

In a recent study of commercial gas reservoirs in the Pannonian and Vienna basins of Hungary and Austria, respectively, Sherwood Lollar et al. (1997) found that the $^3He/CO_2$ ratios were frequently several orders of magnitude greater than the accepted MORB mantle values of 0.15×10^{-9} to 0.5×10^{-9} (Marty and Jambon, 1987; Trull et al., 1993; Marty and Zimmermann, 1999). $^3He/CO_2$ values similarly exceeding MORB have also been reported for high helium wells in USA by Jenden et al. (1993). In the Taranaki Basin, $^3He/CO_2$ values (Table 2) exceed 4.7×10^{-9} in Maui gases and 0.4×10^{-9} in New Plymouth gases indicating a similar depletion of CO_2 relative to ^3He, to that found in the Vienna Basin. Marty and Zimmermann (1999) reported $^3He/CO_2$ ratios of $(0.7\pm0.2)\times10^{-9}$ (corrected for the effects of air-contamination and potential fractional degassing) for N-MORB samples. However, Nishio et al. (1999) reported $^3He/CO_2$ ratios of $(3.5\pm1)\times10^{-9}$ for Rodrigues Triple Junction Indian Ocean MORB and suggested that this higher value reflected 'pristine mantle' whereas lower ratios for MORB indicate carbon recycling to the mantle. Irrespective of the difference between MORBs from the Indian Ocean and from other ocean

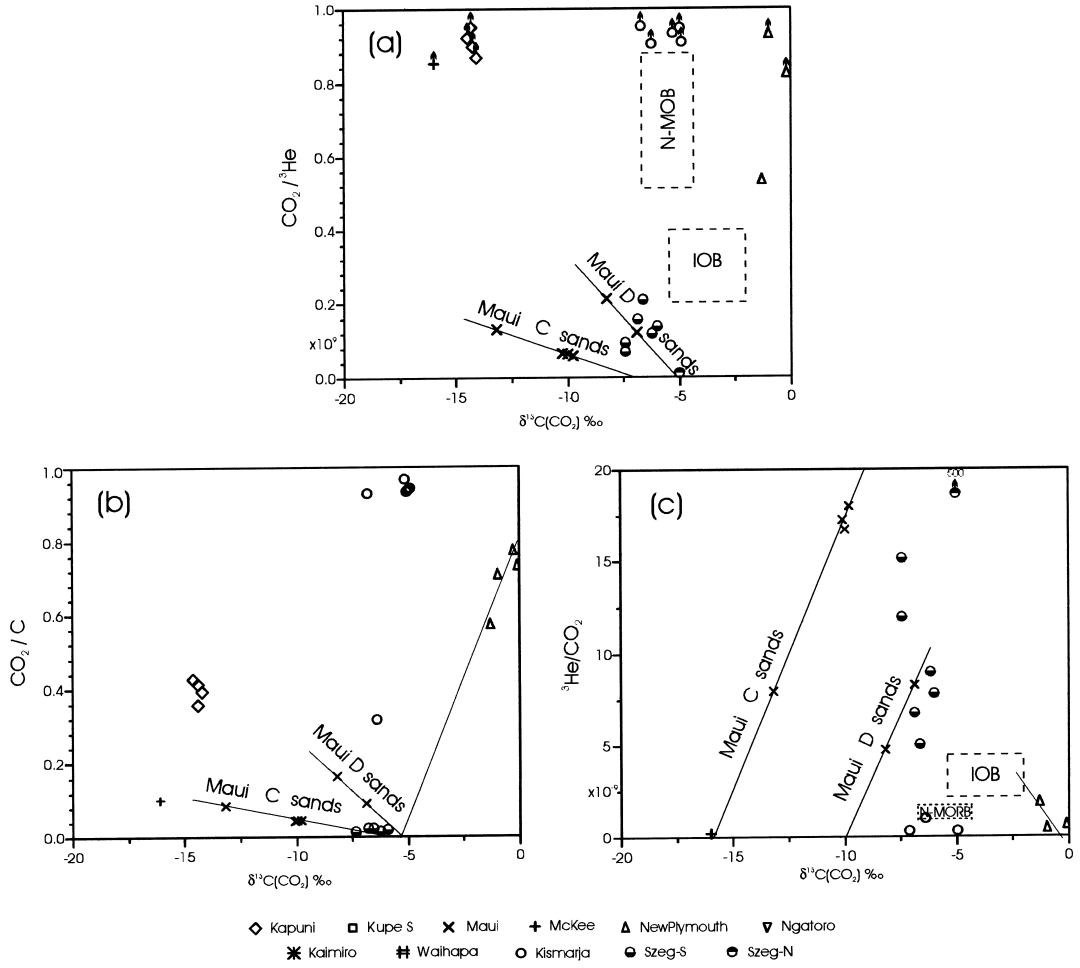

Fig. 4. (a) $CO_2/^3He$ vs. $\delta^{13}C(CO_2)$ for the Taranaki Basin data together with the Sherwood Lollar et al. (1997) data for the Kismarja and Szeg fields of the Pannonian basin. In the Maui field $CO_2/^3He$ ratios are approximately one tenth of the range characteristic of N-MORB (Marty and Zimmermann, 1999) and approximately one third of the range for Indian Ocean MORB reported by Nishio et al. (1999). (b) CO_2/C vs. $\delta^{13}C(CO_2)$ indicates that the mantle isotopic signal is visible at low CO_2 concentrations at between −5 and −7‰ for Maui C, Maui D and New Plymouth similar to that found in Szeg-S and Kismarja. (c) $^3He/CO_2$ vs. $\delta^{13}C(CO_2)$, indicates non-mantle components, at vanishingly small ^3He, of $\delta^{13}C(CO_2)$ between −1 and 0‰ for New Plymouth suggesting a carbonate source, and −16‰ for Maui C sands similar to the −14.5‰ value for Kapuni suggesting an organically influenced source. The Maui D sand samples, however, extrapolate to c.−10‰.

basins, the Maui gases have significantly higher $^3He/CO_2$ ratios compared to any of these MORB estimates indicating a loss of CO_2 by some, as yet unknown mechanism. Sherwood Lollar et al. (1997) considered loss of mantle CO_2 due to possible sinks, including precipitation as carbonate, reduction to graphite, etc., but their suggestions are not fully consistent with the available chemical and isotopic data in hydrocarbon systems.

In order to investigate the role of mantle, crustal and organic carbon on the CO_2 phase in Taranaki Basin, we have plotted, in Fig. 4, $\delta^{13}C(CO_2)$ against (a) $CO_2/^3He$, (b) CO_2/C and (c) $^3He/CO_2$. For comparison the MORB range and those Pannonian Basin data of Sherwood Lollar et al. (1997) that included $\delta^{13}C(CO_2)$ values, are also shown. Fig. 4 illustrates the loss of CO_2 that has occurred in the Maui field — $CO_2/^3He$ ratios are one quarter of the range characteristic of MORB. $\delta^{13}C(CO_2)$ values trend between −5 and −7‰ for Maui C, Maui D and New Plymouth samples at low CO_2/C ratios [Fig. 4(b)] and for Maui samples at low $CO_2/^3He$ ratios [Fig. 4(a)], indicating a very low concentration of MORB derived CO_2 in these wells. Giggenbach (1997) evaluated fluid equilibrium conditions for the Taranaki gases using $FeO/FeO_{1.5}$ mineral buffers and concluded that the system has an overall high redox potential. This would suggest precipitation of carbonate as a more likely cause of the loss of MORB CO_2 than reduction to CH_4. That three of the Taranaki fields shown in Fig. 4(b) extrapolate to similar $\delta^{13}C(CO_2)$ values from both more positive and more negative values further suggests isotopic equilibrium with CH_4 (cf. Giggenbach, 1997) is not a factor in these wells.

Sano and Marty (1995), in their study of the origin of carbon in fumarolic gas from island arcs, took a similar approach to that used in Fig. 4(a) and (c) above. Their plot of $\log(CO_2/^3He)$ against $\delta^{13}C(CO_2)$ however showed $CO_2/^3He$ values considerably exceeding MORB, whereas the Maui, and possibly the New Plymouth samples, in this paper, are significantly depleted in CO_2 compared to MORB.

The isotopic composition of the non-mantle CO_2 in those samples should display vanishingly low ^3He concentrations which have been estimated by plotting $^3He/CO_2$ against $\delta^{13}C(CO_2)$ [Fig. 4(c)]. As indicated, the New Plymouth non-mantle component has a $\delta^{13}C(CO_2)$ value between −1 and 0‰, suggestive of a carbonate source, whereas $\delta^{13}C(CO_2)$ of −16‰ for Maui C sands and −14.6‰ for Kapuni indicates an organically-influenced source. The Maui D sand samples, however, extrapolate to c. −10‰. This may represent a mixture of 30% marine carbonate CO_2 and 70% organic carbon of isotopic composition similar to that previously found at Maui C and Kapuni or may represent a CO_2 contribution from heated greywacke basement (Hulston, 1998). The difference between the isotopic compositions of the CO_2 in the Maui C and New Plymouth sources makes it unlikely that the Maui gases originated from a location further to the NW (in the region of the New Plymouth field) as suggested by Haskell (1991).

3.3. The role of radiogenic helium (He_{rad}) and the He_{rad}/C ratio

If it is assumed that the mantle helium component has the typical subduction zone $^3He/^4He$ ratio of 8 R_A, then it is possible to deduct its ^4He contribution from the total ^4He content of the sample and hence to obtain the radiogenic component (He_{rad}) generated by U-Th series

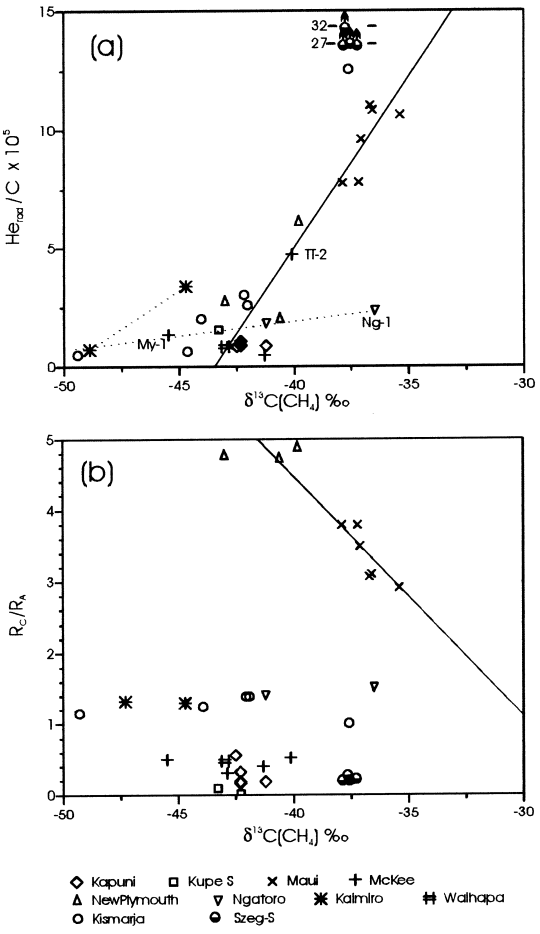

Fig. 5. (a) Plot of He_{rad}/C vs. $\delta^{13}C(CH_4)$ in which the Maui, Kapuni and the majority of the New Plymouth and McKee data appear to follow the straight line relationship intercepting $\delta^{13}C(CH_4)$ between −42 and −43‰ at zero He_{rad}, shown by the solid line, while the Kaimiro and Ngatoro data (dotted) appear to follow lines of lower slope. (b) R_C/R_A vs. $\delta^{13}C(CH_4)$ shows an interesting correlation for the Maui and New Plymouth fields with the more negative $\delta^{13}C(CH_4)$ values corresponding to the highest R_C/R_A values. See text for explanation.

radioactive decay in the sedimentary sands and surrounding formations:-

$$He_{rad} = He_{tot}[1 - (R_C/R_A)/8] \quad (3)$$

The He_{rad} production depends on the time the natural gas has been stored in the basin and on the proportion of the generated He_{rad} released by the U-Th containing material. It also depends on the U and Th content of the sedimentary deposit, which may be assumed to be similar across the Taranaki Basin. Although it might be expected that the He_{rad}/C ratio would be controlled by the rate of release of He_{rad} from the rocks, which in turn correlates with heat flow, the best correlation was found to be between He_{rad}/C and $\delta^{13}C(CH_4)$ [Fig. 5(a)]. In this plot, the Taranaki data with $He_{rad}/C > 4\times10^5$ appear to follow closely ($r = 0.92$) a linear relationship intercepting $\delta^{13}C(CH_4)$ at −43.5‰ at zero He_{rad}/C (solid line). The data with $He_{rad}/C < 4\times10^5$, on the other hand, is more scattered, with all except one point between −40 and −46‰. The Kismarja data shown in Fig. 5(a) show a similar pattern to the Taranaki data, with similar intercept but a slightly higher slope, indicating a similarity of He_{rad} production in these systems. The He_{rad}/C ratio in the Szeg-S field is however three times that in the Maui field despite the similarity in their $\delta^{13}C(CH_4)$ values.

The results shown in Fig. 5(a) suggest that He_{rad}/C is correlated with the maturity of the methane as indicated by the $\delta^{13}C(CH_4)$ values. The open-system pyrolysis experiments of Cramer et al. (1998) showed that between 350 and 700°C the $\delta^{13}C(CH_4)$ value of generated methane increased steadily from c. −40‰ at c. 5% realisable methane potential to −30‰ at c. 90% of realisable methane potential. In the very earliest stages of the pyrolysis, however, more negative $\delta^{13}C(CH_4)$ values were obtained (c. −50‰). Cramer et al. (1998) point out that translation of the kinetic isotope effects to temperatures in natural systems (100–150°C) would widen the range of expected $\delta^{13}C(CH_4)$ values. Therefore the range of $\delta^{13}C(CH_4)$ values found in the Taranaki Basin can be explained without invoking the deep gas abiogenic methane hypothesis of Gold and Soter (1982) as the cause of the more positive $\delta^{13}C(CH_4)$ values found at Maui. The very negative $\delta^{13}C(CH_4)$ values observed for one Kismarja sample and the Kaimiro-5 well (Table 2) may arise from conditions at initial stages of pyrolysis. Alternatively, the younger source rocks in the

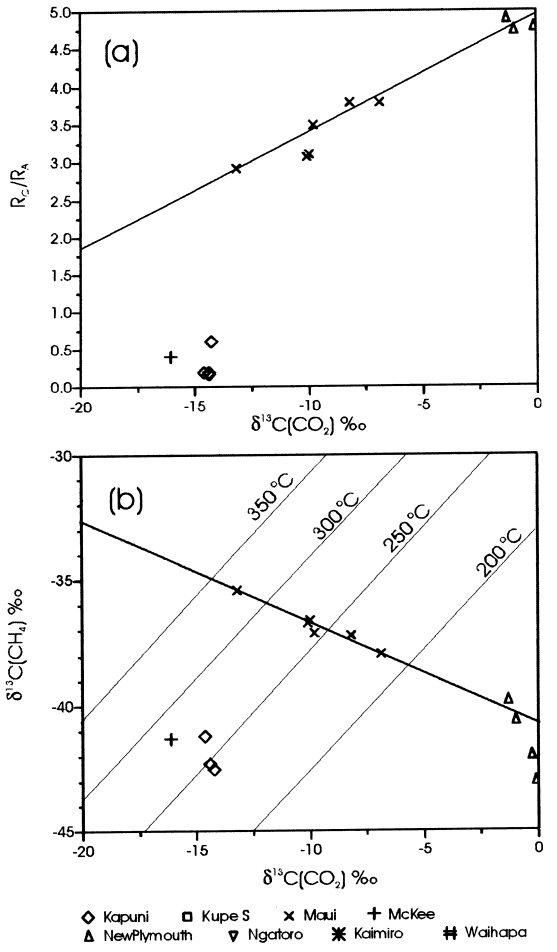

Fig. 6. (a) R_C/R_A vs. $\delta^{13}C(CO_2)$ shows a positive correlation for the Maui and New Plymouth samples. This arises because of the similar He_{rad}/C ratios of these samples and the contributions of mantle and carbonate CO_2 discussed earlier [Fig. 4(b) and (c)]. (b) $\delta^{13}C(CH_4)$ vs. $\delta^{13}C(CO_2)$ provides the most dramatic illustration of an effect in which Maui variations are totally out of sympathy with carbon isotopic equilibrium temperatures shown by the dotted lines.

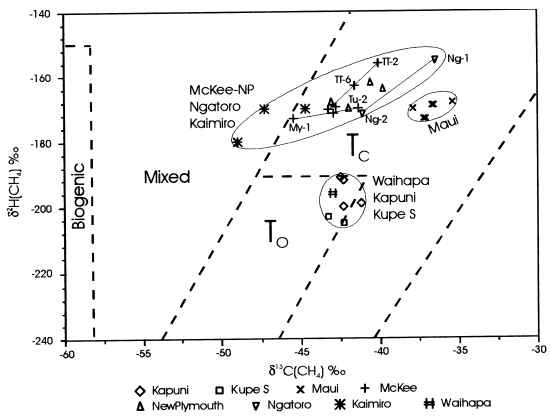

Fig. 7. Schoell genetic characterization diagram of $\delta^2H(CH_4)$ vs. $\delta^{13}C(CH_4)$ shows that the western Taranaki gases plot in the "gas associated with condensate" (T_C) category of Schoell (1983) with some Kaimiro gases tending towards the "mixed" biogenic/condensate category. The eastern Taranaki gases are on the boundary of the "gases associated with petroleum" (T_O) category.

Kaimiro and Ngatoro higher heat flow fields may have reached maturity faster than those at Maui resulting in lower He_{rad} production, and in the lower sloped dotted lines in Fig. 5(a).

3.4. The relationship between R_C/R_A, $\delta^{13}C(CH_4)$ and $\delta^{13}C(CO_2)$ at Maui

For the Maui and New Plymouth fields, more negative $\delta^{13}C(CH_4)$ values correspond to high R_C/R_A [Fig. 5(b)]. This arises because the $^3He/^4He$ ratio is related to the ratio of mantle to radiogenic crustal helium and, as shown in Fig. 3(a), the $^3He/C$ ratios of the Maui gas samples are constant and similar to those of the New Plymouth gas samples. However, as shown in Fig. 5(a), radiogenic crustal helium increases as $\delta^{13}C(CH_4)$ becomes more positive. The negative slope relationship for Maui and New Plymouth fields [Fig. 5(b)] does not appear for the other fields because of the large variation of $^3He/C$ within these fields and because of non-linearity in the He_{rad}/C vs. $\delta^{13}C(CH_4)$ relationship for more negative $\delta^{13}C(CH_4)$ values in Fig. 5(a). R_C/R_A vs. $\delta^{13}C(CO_2)$ [Fig. 6(a)] displays a positive correlation for the Maui and New Plymouth samples. This arises because of (i) the similar He_{rad}/C ratios of these samples and (ii) the contributions of mantle and carbonate CO_2 discussed earlier [Fig 4(b) and (c)]. Since we have already noted that R_C/R_A trends positively with surface heat flow, we can now understand the positive trend shown between $\delta^{13}C(CO_2)$ and surface heat flow shown in Fig. 3(c).

Fig. 6(b) indicates a negative correlation between $\delta^{13}C(CH_4)$ and $\delta^{13}C(CO_2)$ for the Maui data. However this correlation cannot to be due to carbon isotopic equilibrium effects, because Δ [$\delta^{13}C(CH_4)-\delta^{13}C$ (CO_2)] data would represent isotopic equilibrium temperatures (Lyon and Hulston, 1984) of 215°C (D sand), 260°C (C

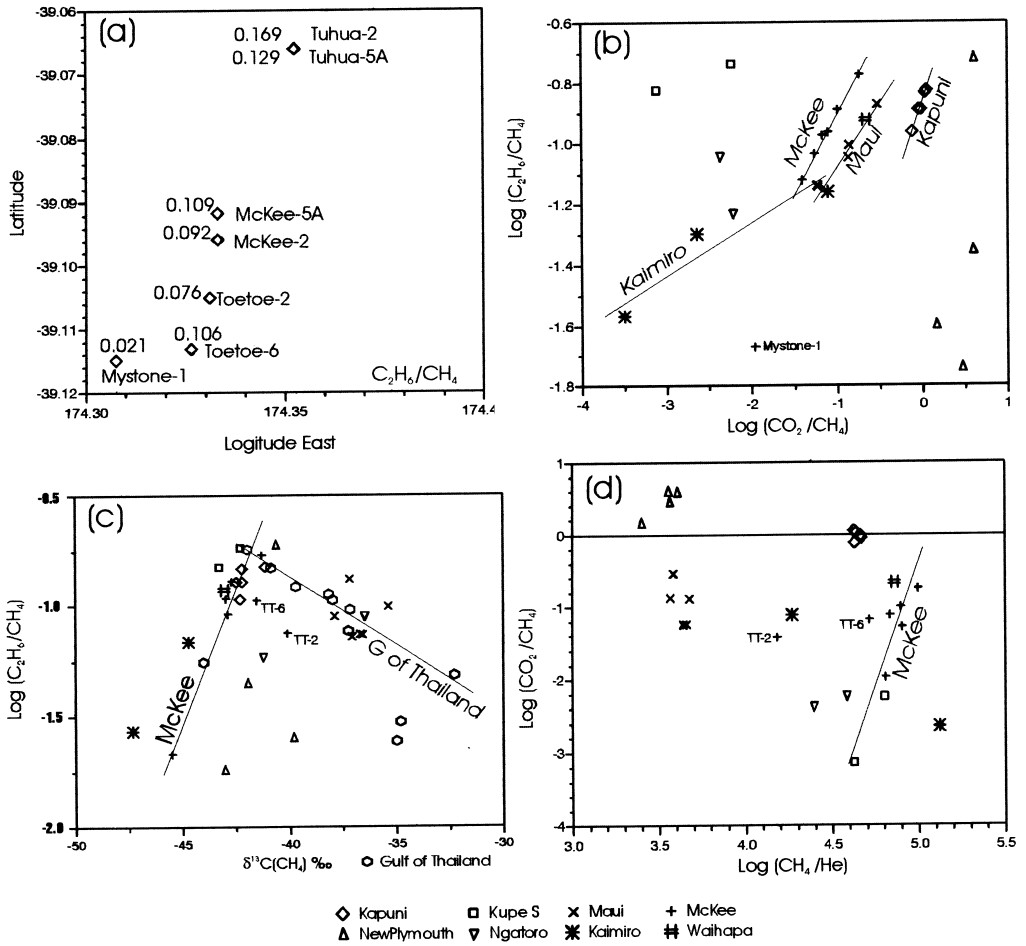

Fig. 8. Plots relating to the variation of (a) C_2H_6/CH_4 across the McKee field; of $\log(C_2H_6/CH_4)$ with (b) $\log(CO_2/CH_4)$ and (c) $\delta^{13}C(CH_4)$ and of (d) $\log(CO_2/CH_4)$ vs. $\log(CH_4/He)$ within fields in the basin. For comparison Gulf of Thailand data (Giggenbach, 1997) has been plotted in (c) to illustrate the effect of the maturation process.

sand and Kapuni) and 325°C for one C sand gas, all of which are unreasonably high. Giggenbach (1997) concluded that the time required for isotopic equilibrium to be established is many times greater than that for chemical equilibrium between CO_2 and CH_4. It would therefore appear more likely that the carbon isotopic values of CO_2 and CH_4 are controlled by two independent processes, both of which correlate to R_C/R_A [see Figs. 5(b) and 6(a)]. $\delta^{13}C$ of both CO_2 and CH_4 may represent mixing curves of pyrolytic methane at various maturation levels, mixed with pyrolytic and marine equilibrated CO_2 (with $\delta^{13}C = 0$). The New Plymouth samples display very low pyrolytic CO_2.

3.5. Hydrocarbon chemistry and isotopic compositions

Distinct differences are apparent in the chemical and isotopic composition of the gases from Maui, Kapuni and Kupe South fields (Tables 2 and 3). Maui gas is wet, containing almost 10% ethane and higher hydrocarbons, with small quantities of CO_2 and N_2. The iso/*n*-butane ratio (< 1.0) indicates a mature gas, and the methane is isotopically enriched in ^{13}C compared to other deep sedimentary methane such as from the Permian Basin of West Texas. Stahl and Carey (1975), Stahl (1977) and Schoell (1983) have established a relationship between methane $\delta^{13}C$, gas wetness, and maturity of the gas source: in commercial gas accumulations, a progressive increase in source maturity results in drier gases with isotopically heavy methane. Schoell (1983) has extended this observation to a generic characterization scheme based on gas wetness, methane $\delta^{13}C$ and δ^2H, and ethane $\delta^{13}C$. Kapuni gas has similar wetness to Maui gas, but is much richer in CO_2, which, based on the light carbon isotope value ($\delta^{13}C$ −14.5‰), appears to be at least partially derived from decomposition of organic matter. Kupe South gas, on the other hand, is wetter and contains virtually no CO_2. Kapuni and Kupe South gases both appear to be less mature than Maui gas as reflected in the higher iso/*n*-butane ratio (> 1.0) and the lighter methane $\delta^{13}C$ value (−42.6‰). The Taranaki gases are plotted on the generic characterization diagram of Schoell (Fig. 7). The western Taranaki gases fall within the regime of the "gas associated with condensate" (T_C) category of Schoell (1983) with some Kaimiro gases tending towards the "mixed" biogenic/condensate category. The eastern Taranaki gases are on the boundary of the "gases associated with petroleum" (T_O) category. The variation in $\delta^2H(CH_4)$ is similar to that expected from the Schoell trend line, relative to the variation in $\delta^{13}C(CH_4)$, but the data form three clusters (Fig. 7). As noted in Fig. 3(d) there is a distinct difference in $\delta^2H(CH_4)$ between the Kupe-Kapuni-Waihapa fields and other Taranaki field to the west. This may relate to heat flow or temperature, but the relatively sudden change is surprising. Alternately it may relate to differences in the proportions of marine and terrestrial source rocks, which Killops et al. (1994) distinguished for the Kapuni, McKee and Maui groups on the basis of biomarker studies (see Fig. 2) even though the results in Fig. 2 refer to oils while those in Fig. 7 refer to gases. Giggenbach (1997) failed to find a correlation between $\delta^{13}C(CH_4)$ and $\delta^2H(CH_4)$ similar to that obtained for pyrolysis of xylite coal by Berner et al. (1995) in which $\delta^2H(CH_4)$ increased with maturity without significant change in $\delta^{13}C(CH_4)$. The results in this study display a 4:1 change in $\delta^2H(CH_4)$ vs. $\delta^{13}C(CH_4)$ for Toetoe and Ngatoro, however the remaining McKee field samples and the New Plymouth samples show a slope c. 1, implying some process other than maturation is affecting these results, probably the nature of the source material.

3.6. The relationships between C_2H_6/CH_4, CO_2/CH_4 and $\delta^{13}C(CH_4)$ within fields

Although a significant correlation between $\log(C_2H_6/CH_4)$ and surface heat flow is indicated in Fig. 3(e), several fields show outlier $\log(C_2H_6/CH_4)$ values. In the McKee field, which has the greatest spread, C_2H_6/CH_4 values were observed to increase from SSW to NNE across the field [Fig. 8(a)]. Although no data on heat flow variations across the field are available, it is unlikely that they would vary significantly. However, there is a significant correlation between $\log(C_2H_6/CH_4)$ and $\log(CO_2/CH_4)$ as shown in Fig. 8(b).[2] With the exception of Ngatoro and New Plymouth fields, the trend is for CO_2 and C_2H_6 to increase together relative to CH_4. The maturity process for Taranaki coals (Killops et al., 1996) indicates successive production peaks in CO_2, wet gas and finally CH_4 production as the maturity (and rank) increases. Thus, in the later stages of maturity, it would be expected that CO_2 and C_2H_6 would decrease and CH_4 would increase leading to a relationship of the type shown in Fig. 8(b).

The trend observed in Fig. 8(c) is partly a function of the type of starting organic matter (kerogen) and partly the maturation level of the kerogen (Rohrback et al., 1984). The McKee and Kaimiro gas samples generally appear immature and because the kerogen is land plant in origin the C_2H_6/CH_4 ratio is low. This ratio increases in Kapuni and Kupe S. samples which approach a point of early maturity. The Maui (and Gulf of Thailand shown for comparison) gas samples are derived from mature kerogen. The Maui samples also contain a larger component of marine derived Type II kerogen.

[2] Although the range of C_2H_6/CH_4 values observed in Fig. 8(b) is sufficent to distinguish between logarithmic and linear relationships, the correlation with $\log(CO_2/CH_4)$ was found to be much more significant than that with CO_2/CH_2, particularly for the McKee field.

For McKee (excluding Toetoe) and Kaimiro source rocks, the maturation process begins initially with generation of CH_4 and with increase in time and temperature, C_2H_6 and other "wet" gases form. This results in a positive slope to the curve. When maturation has progressed, as is observed for the Maui and Gulf of Thailand gas samples,

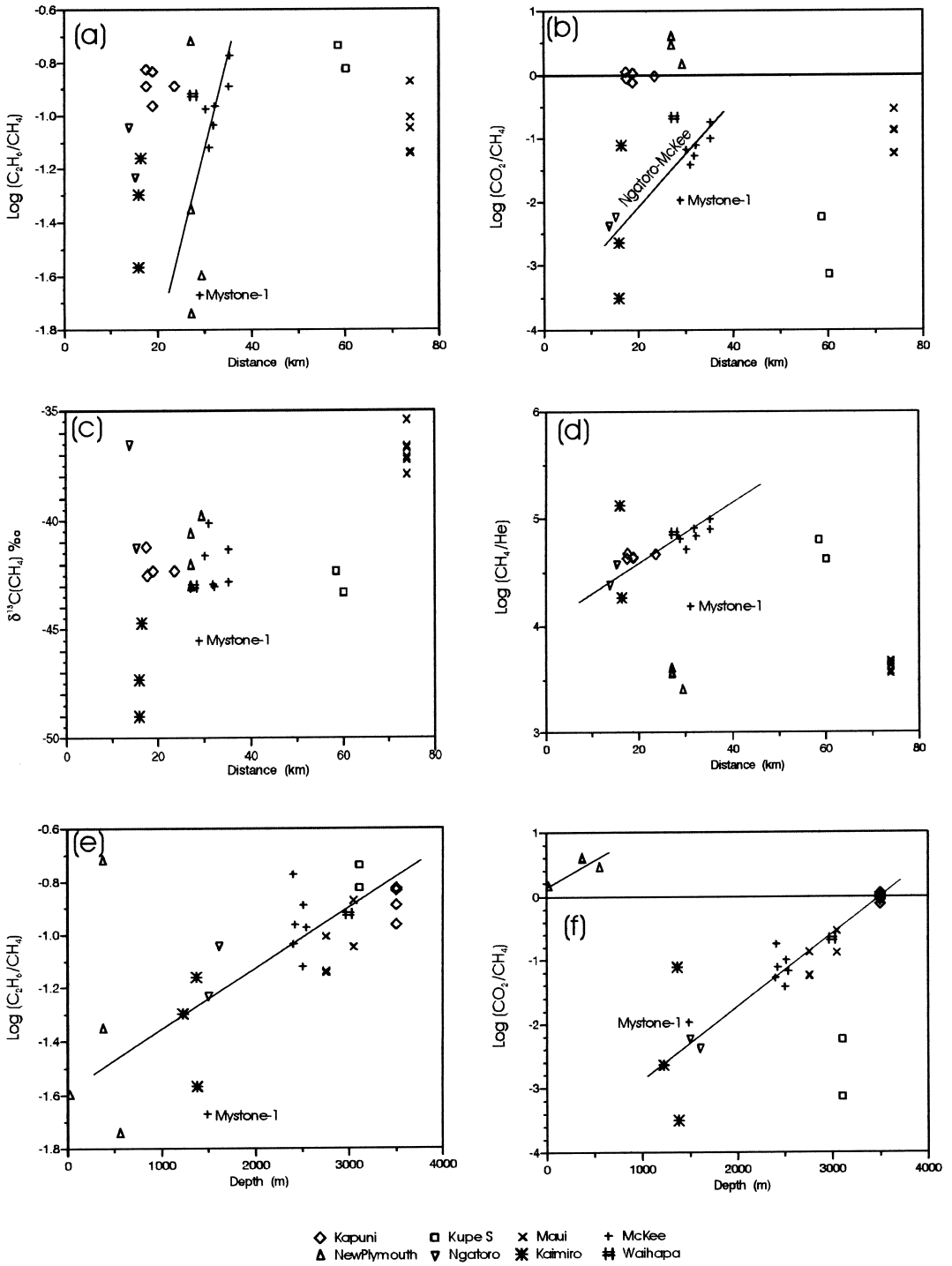

Fig. 9. Variations with depth of the reservoir and with distance from Mt Taranaki of (a,e) $\log(C_2H_6/CH_4)$, (b,f) $\log(CO_2/CH_4)$, (c,g) $\delta^{13}C(CH_4)$ and (d,h) $\log(CH_4/He)$ (*continued on next page*).

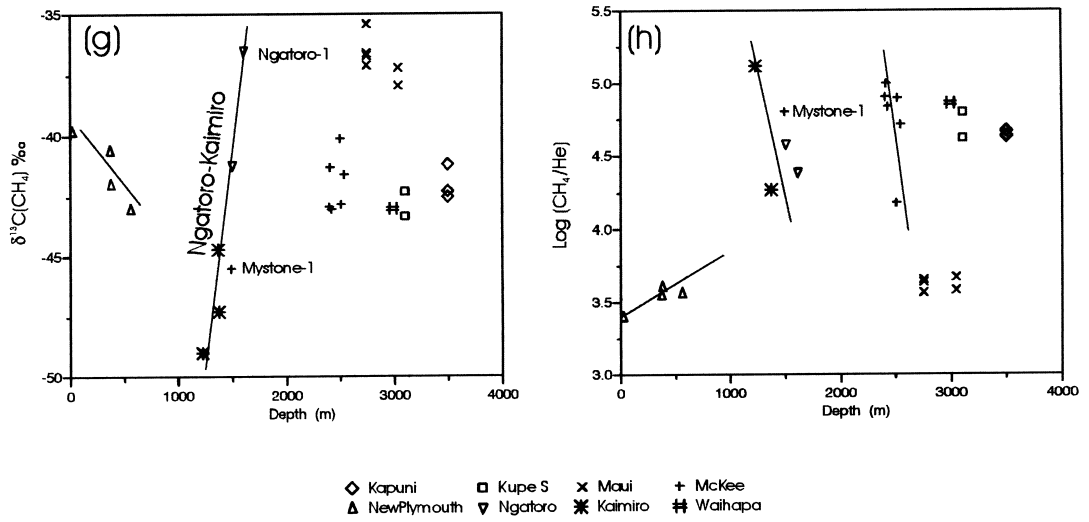

Fig. 9. (*continued*).

the "wet" gases begin to crack and form methane. Hence, the C_2H_6 to CH_4 ratio begins to decrease.

An alternative explanation for these effects relates to the widely differing solubility of CO_2, C_2H_6, CH_4 and He, which would be relevant if groundwater flow was occurring between wells of a field or between adjacent fields. The slope of $\log(CO_2/CH_4)$ vs. $\log(CH_4/He)$ [Fig. 8(d)] for the majority of the McKee samples is close to that expected from solubility data but the Toetoe data (TT-2, TT-6) indicates a lower slope, possibly due to the addition of radiogenic He.

3.7. Possible geographic effects relative to Mt Taranaki

Allis et al. (1997) estimate that 3.8 million m^3/day of meteoric recharge arises from rainfall on the volcanic cone and ring plain of Mt Taranaki with maximum flow velocities of 8 cm/day occurring in the northeast and southeast. Modelling indicated that this flow extends at least to the Kaimiro and Ngatoro fields in the north and to the Kapuni field in the southeast. This is confirmed by a measured water head gradient southwards of 4–8 m/km across the Kapuni field reservoir. In order to find if this groundwater flow is influencing the gas compositions, we have plotted in Fig. 9 the parameters, $\log(C_2H_6/CH_4)$, $\log(CO_2/CH_4)$, $\delta^{13}C(CH_4)$ and $\log(CH_4/He)$ against the distance from Mt. Taranaki and the depth of gasflow from the well. It can be seen from these plots that at least some parameters appear to be related to distance for wells within 35 km in all directions except the west where the limit appears to be c. 20 km. Thus, groundwater may be having an influence in carrying the more soluble CO_2 and C_2H_6 gases away from the mountain and to greater depths.

The depth plots show other relationships that may not be due to solubility effects. In particular Fig. 9(g), between $\delta^{13}C(CH_4)$ and depth, shows a consistent trend for the Ngatoro-Kaimiro wells whereas in all other $\delta^{13}C(CH_4)$ plots shown in this paper, the results from these wells tend to scatter away from the main trend lines.

3.8. Relevance to the geology and geophysics of Taranaki Basin

Correlations among $^3He/^4He$, He_{rad}/C and carbon isotopes are stronger for the Maui field (Fig. 3) than correlations of these parameters with surface heat flow. We need, therefore, to re-examine the likely relationships between surface heat flow and (i) mantle helium contribution and (ii) the maturity of the hydrocarbon generation process. The observed relationship between heat and ^3He release in geothermal systems reported by Jenkins et al. (1978) and Lupton (1983) is 2×10^{-6} to 4×10^{-7} Joules/^3He atom. Hulston and Lupton (1996) obtained similar values in the Taupo Volcanic Zone, but found variations exceeding a factor of two. In this case, the mantle helium flux may come from direct leakage from the mantle or through outgassing of local igneous intrusions forming geothermal circulation systems and not necessarily from regional heat. If this is correct, the basal heat flow calculated for the Taranaki Basin by Armstrong and Chapman (1998) are not directly applicable to this work. However, the concepts outlined in their paper do have application, particularly the perturbation of the surface heat flow by groundwater fluidflow. The maturity of the hydrocarbon generation process is, however, a product of time and temperature and

thus requires knowledge of past temperatures and depths of burial. Some of the information required for this calculation has been obtained in the investigations of the Taranaki Basin by the Institute of Geological & Nuclear Sciences in New Zealand (e.g. King and Thrasher, 1996) but as these data would still only provide an improved estimate, it was considered beyond the scope of this paper. We believe that our use of present surface heat flow still provides a reasonable approximation to the two processes listed above.

4. Conclusions

The main findings from this study are as follows:

1. The contribution of mantle helium to Taranaki Basin fluids increases from near zero in the eastern fields to a maximum in the Maui and New Plymouth fields on the western margin of the basin.
2. The mantle helium contribution correlates with the variation in present surface heat flow (from 50 mWm^{-2} in the east to 65–75 mWm^{-2} in the west)-corresponding to thinning and increased faulting of the lithosphere in an east to west direction.
3. The carbon isotopic composition of the CO_2 in the Maui and New Plymouth fields indicates a mixture of organically sourced CO_2, marine carbonate CO_2 and mantle CO_2.
4. The carbon isotope composition of the CH_4 component varies from −49 to −35‰ corresponding mainly with increasing maturity of the hydrocarbon process.
5. The maturity, which relates both to the age of the source rocks (confirmed by the high radiogenic $^4He/C$ ratio) and to surface heat flow, is highest in the Maui field where the $\delta^{13}C(CH_4)$ values reach a maximum of −35.4‰.
6. In general the hydrocarbons in the lower heatflow areas have relatively lower CH_4 and are wetter (viz. have higher C_2H_6/CH_4 ratios) than those in the higher heat flow regions. This would appear to relate to an increase in CH_4 production relative to C_2H_6 at the increased temperatures found in the higher heat flow areas.
7. Within-field variations of $\log(C_2H_6/CH_4)$ correlate with $\log(CO_2/CH_4)$ to a much greater extent than expected from maturity effects. In contrast, the slope of the $\log(C_2H_6/CH_4)$ v $\delta^{13}C(CH_4)$ plot is positive in many fields which is the opposite of that expected during early stages of maturation.
8. Within the area of influence of the Mt Taranaki groundwater system, some gas ratios show correlations with distance from the mountain and with depth of the gas reservoir, possibly reflecting gas–water interactions.
9. Differences in $\delta^2H(CH_4)$ among the various fields may be due to variations in the proportion of marine and terrestrial origins of the Taranaki source materials as indicated by biomarker distributions (Killops et al., 1994).
10. No evidence to support a significant addition of deep-earth abiogenic methane was found.

The relatively high R_C/R_A values for the Maui and New Plymouth Fields would be expected to decrease considerably in time due to the addition of radiogenic ^4He. Thus many older hydrocarbon basins in the world formed along tectonically active margins may initially have had similar high R_C/R_A values to those currently found in the Taranaki Basin during their early gas-forming history.

Acknowledgements

We thank Shell Todd Oil Services (STOS) and TCPL Ltd. for respective provision of the Maui and Kapuni samples and Kupe South well samples. Alan Jefferey and Robert Poreda provided analytical expertise, and we acknowledge Harmon Craig for advice and access to helium isotope mass spectrometer facilities at the SIO Isotope Laboratory. Assistance and advice from Steve Killops and other colleagues at the N.Z. Institute of Geological & Nuclear Sciences has been appreciated. Funding from the NZ Foundation for Research and Technology under contract No. C05807 is acknowledged by the first author.

References

Adams, R.D., Ware, D.E., 1977. Subcrustal earthquakes between New Zealand: Locations determined with a laterally inhomogeneous velocity model. N.Z. J. Geol. Geophy. 20, 59–83.

Allis, R.G., Armstrong, P.A., Funnell, R.H., 1995. Implications of a high heat flow anomaly around New Plymouth, North Island, New Zealand. N.Z. J. Geol. Geophy. 38, 121–130.

Allis, R.G., Zhan, X., Evans, G., Kroopnick, P., 1997. Groundwater flow beneath Mt Taranaki, New Zealand, and implications for oil and gas migration. N.Z. J. Geol. Geophy 40, 137–149.

Armstrong, P.A., Chapman, D.S., 1998. Beyond surface heat flow: An example from a tectonically active sedimentary basin. Geology 26, 183–186.

Armstrong, P.A., Chapman, D.S., Funnell, R.H., Allis, R.G., Kamp, P.J.J., 1996. Thermal modelling and hydrocarbon generation in an active-margin basin: Taranaki Basin, New Zealand. AAPG Bull. 80, 1216–1241.

Berner, U., Faber, E., Scheeder, G., Panten, D., 1995. Primary cracking of algal and landplant kerogens: kinetic models of

isotope variations in methane, ethane and propane. Chem. Geol. 126, 233–245.

Cramer, B., Krooss, B.M., Littke, R., 1998. Modelling isotopic fractionation during primary cracking of natural gas: a kinetic approach. Chem. Geol. 149, 235–250.

Darling, W.G., 1998. Hydrothermal hydrocarbon gases: 1, genesis and geothermometry. Applied Geochemistry 13, 815–824.

Funnell, R., Chapman, D., Allis, R., Armstrong, P., 1996. Thermal state of the Taranaki Basin, New Zealand. J. Geoph. Res. 101 (B11), 197–215.

Giggenbach, W.F., 1997. Relative importance of thermodynamic and kinetic processes in governing the chemical and isotopic composition of carbon gases in high-heat flow sedimentary basins. Geochim. Cosmochim. Acta 61, 3763–3785.

Giggenbach, W.F., Sano, Y., Wakita, H., 1993. Isotopic composition of helium and CO_2 and CH_4 contents in gases produced along the New Zealand part of a convergent plate boundary. Geochim. Cosmochim. Acta 57, 3427–3455.

Gold, T., Soter, S., 1982. Abiogenic methane and the origin of petroleum. Energy Explor. Exploit. 1, 89–104.

Haskell, T., 1991. An analysis of Taranaki Basin hydrocarbon migration paths — some questions answered. Petrol. Explor. New Zealand News 27, 19–25.

Hilton, D.R., Craig, H., 1989. The Siljan deep well: helium isotope results. Geochim. Cosmochim. Acta 53, 3311–3316.

Hulston, J.R., Lupton, J.E., 1996. Helium isotope studies of geothermal fields in the Taupo Volcanic Zone, New Zealand. J. Volcan. Geotherm. Res. 74, 297–321.

Hulston, J.R., 1998. Correlations between B/Cl ratios and other chemical and isotopic components of Taupo Volcanic Zone, NZ geothermal fluids — evidence for water–rock interaction as a major source of boron and gas. In: Arehart, G.B., Hulston, J.R. (Eds.), Proc 9th Intnl Symp. on Water–Rock Interaction. Balkema, Rotterdam, pp. 629–632.

Jenden, P.D., Kaplan, I.R., 1989. Origin of natural gas in the Sacramento basin, California. American Association of Petroleum Geologists Bulletin 73, 431–453.

Jenden, P.D., Hilton, D.R., Kaplan, I.R., Craig, H., 1993. Abiogenic hydrocarbons and mantle helium in oil and gas fields. In: Howell, D.G. (Ed.), The Future of Energy Gases. US Geological Survey Professional Paper 1570, pp. 31–56.

Jenkins, W.J., Edmond, J.M., Corliss, J.G., 1978. Excess ^{3}He and ^{4}He in Galapagos submarine hydrothermal waters. Nature 272, 156–158.

Killops, S.D., Allis, R.G., Funnell, R.H., 1996. Carbon dioxide generation from coals in the Taranaki Basin, New Zealand: implications for petroleum migration on southeast Asian Tertiary basins. AAPG Bull 80, 545–569.

Killops, S.D., Woolhouse, A.D., Weston, R.J., Cook, R.A., 1994. A geochemical appraisal of oil generation in the Taranaki Basin, New Zealand. AAPG Bulletin 78, 160–1585.

King, P.R., Thrasher G.P., 1996. Cretaceous–Cenozoic geology and petroleum systems of the Taranaki Basin, New Zealand. Institute of Geological & Nuclear Sciences Monograph 13 (six enclosures). Lower Hutt, New Zealand.

Lupton, J.E., 1983. Terrestrial inert gases: Isotope tracer studies and clues to primordial components in the mantle. Ann. Rev. Earth Planet. Sci. 11, 371–414.

Lyon, G.L., Giggenbach, W.F., Sano, Y., 1996. Variations in the chemical and isotopic composition of Taranaki gases and their possible causes. New Zealand Petroleum Conf. 1, 171–174.

Lyon, G.L., Hulston, J.R., 1984. Carbon and hydrogen isotopic compositions of New Zealand geothermal gases. Geochim. Cosmochim. Acta 48, 1161–1171.

McBeath, D.M., 1977. Gas-condensate fields of the Taranaki basin, New Zealand. N.Z. J. Geol. Geophy. 20, 99–127.

Marty, B., Jambon, A., 1987. C/^{3}He in volatile fluxes from the solid Earth: implications for carbon geodynamics. Earth. Planet. Sci. Lett. 83, 16–26.

Marty, B., Zimmermann, L., 1999. Volatiles (He, C, N, Ar) in mid-ocean ridge basalts: assessment of shallow-level fractionation and characterization of source composition. Geochim. Cosmochim. Acta 63, 3619–3633.

Nishio, Y., Ishii, T., Gamo, T., Sano, Y., 1999. Volatile element isotopic systematics of Rodrigues Triple Junction Indian Ocean MORB: implications for mantle heterogeneity. Earth. Planet. Sci. Lett. 170, 241–253.

Pilaar, W.F.H., Wakefield, L.L. 1978. Structural and stratigraphic evolution of the Taranaki Basin, offshore North Island, New Zealand. Australian Petroleum Exploration Assoc Journal XX, 93-101.

Pilaar, W.F.H., Wakefield L.L., 1984. Hydrocarbon generation in the Taranaki Basin, New Zealand. In: Demaison, G., Murris, R.J. (Eds.). Petroleum Geochemistry and Basin Evaluation , AAPG Memoir 35, 405-423.

Poreda, R.J., Jenden, P.D., Kaplan, I.R., Craig, H., 1986. Mantle helium in Sacramento basin natural gas wells. Geochim. Cosmochim. Acta 50, 2847–2853.

Poreda, R.J., Jefferey, A.W.A., Kaplan, I.R., Craig, H., 1988. Magmatic helium subduction-zone natural gases. Chem. Geol. 71, 199–210.

Rohrback, B.G., Peters, K.E., Kaplan, I.R., 1984. Geochemistry of artificially heated humic and sapropelic sediments — II. Oil and gas generation. AAPG Bull 68, 911–970.

Sano, Y., Marty, B., 1995. Origin of carbon in fumarolic gas from island arcs. Chem. Geol. 119, 265–274.

Sano, Y., Wakita, H., Giggenbach, W.F., 1987. Island arc tectonics of New Zealand manifested in helium isotope ratios. Geochim. Cosmochim. Acta 51, 1855–1860.

Schoell, M., 1983. Genetic characteristics of natural gases. AAPG Bull 67, 2225–2238.

Sherwood Lollar, B., Ballentine, C.J., O'Nions, R.K., 1997. The fate of mantle-derived carbon in a continental sedimentary basin: integration of C/He relationships and stable isotope signatures. Geochim. Cosmochim. Acta 61, 2295–2307.

Stahl, W.J., 1977. Carbon and nitrogen isotopes in hydrocarbon research and exploration. Chem. Geol. 20, 121–149.

Stahl, W.J., Carey, B.D., 1975. Applications of carbon isotope data in exploration work. Chem. Geol. 16, 257–267.

Stern, T.A., Davey, F.J., 1990. Deep seismic expression of a foreland basin: Taranaki basin, New Zealand. Geology 18, 979–982.

Trull, T., Nadeau, S., Pineau, F., Polve, M., Javoy, M., 1993. C-He systematics in hotspot xenoliths: implications for mantle carbon contents and carbon recycling. Earth Planet. Sci. Lett. 118, 43–64.